

Review

The Underexplored Field of Lanthanide Complexes with Helicene Ligands: Towards Chiral Lanthanide Single Molecule Magnets

Gabriela Handzlik *, Katarzyna Rzepka and Dawid Pinkowicz *

Faculty of Chemistry, Jagiellonian University, Gronostajowa 2, 30-387 Kraków, Poland; katarzyna01.rzepka@student.uj.edu.pl

* Correspondence: gabriela.handzlik@uj.edu.pl (G.H.); dawid.pinkowicz@uj.edu.pl (D.P.)

Abstract: The effective combination of chirality and magnetism in a single crystalline material can lead to fascinating cross-effects, such as magneto-chiral dichroism. Among a large variety of chiral ligands utilized in the design and synthesis of chiral magnetic materials, helicenes seem to be the most appealing ones, due to the exceptionally high specific rotation values that reach thousands of $\text{deg}\cdot\text{cm}^3\cdot\text{g}^{-1}\cdot\text{dm}^{-1}$, which is two orders of magnitude higher than for compounds with chiral carbon atoms. Despite the sizeable family of transition metal complexes with helicene-type ligands, there are only a few examples of such complexes with lanthanide ions. In this mini-review, we describe the most recent developments in the field of lanthanide-based complexes with helicene-type ligands and summarize insights regarding the further exploration of this family of compounds towards multifunctional chiral lanthanide single molecule magnets (Ln-SMMs).



Citation: Handzlik, G.; Rzepka, K.; Pinkowicz, D. The Underexplored Field of Lanthanide Complexes with Helicene Ligands: Towards Chiral Lanthanide Single Molecule Magnets. *Magnetochemistry* **2021**, *7*, 138. <https://doi.org/10.3390/magnetochemistry7100138>

Academic Editors: Marius Andruh, Eva Rentschler and Andrea Caneschi

Received: 3 September 2021

Accepted: 30 September 2021

Published: 9 October 2021

Publisher's Note: MDPI stays neutral with regard to jurisdictional claims in published maps and institutional affiliations.



Copyright: © 2021 by the authors. Licensee MDPI, Basel, Switzerland. This article is an open access article distributed under the terms and conditions of the Creative Commons Attribution (CC BY) license (<https://creativecommons.org/licenses/by/4.0/>).

Keywords: helicenes; lanthanides; chirality; molecular magnetism; magneto-chiral dichroism; magnetic circular dichroism; circular dichroism; circularly polarized luminescence

1. Introduction

Helicenes are fascinating molecules with inherent chirality arising from the screw shape of their ortho-fused polycyclic skeleton. This nonplanar skeleton exhibits axial chirality, which is configurationally stable for at least five fused rings [1]. Similar to other polycyclic aromatic compounds, helicenes are considered as potential components of molecular electronics and photonics, due to their unique delocalized electronic structure. Moreover, helicenes can be decorated with various functional groups, which has been reported widely since the 1950s [2–4]. Rational selection of these groups makes the helicene a truly multifunctional ligand suitable for coordination to various metal ions, yielding classical coordination complexes as well as organometallic compounds [5]. The main advantage of helicenes as chiral ligands is their huge specific rotation, which is as much as two orders of magnitude larger than for compounds with chiral carbon atoms, such as glucose or camphor [6,7]. Moreover, helicenes often show spectacular emission properties [8–12]. If pure helicene enantiomers are exploited in the synthesis of lanthanide complexes, a co-existence or coupling of exceptional optical activity and slow relaxation of the magnetization in the resulting complexes can be anticipated. Hence, the efficient merging of the chirality of helicenes and the magnetism of lanthanide ions in a single molecule can lead to the observation of very rare magneto-chiral cross-effects at the molecular level, resulting in truly multifunctional molecular devices.

Lanthanides are widely studied in the field of molecular magnetism due to their potential applications as single molecule memory elements (single molecule magnets; SMMs) [13], quantum computing units (molecular qubits) [14] and spin valves and sensors [15]. These applications are possible due to the strong intrinsic magnetic anisotropy of lanthanide ions, caused by strong spin-orbit coupling (SOC). The magnetic anisotropy can

be fine-tuned by manipulating the crystal field of the carefully designed ligand scaffolds, in conformity with the oblate/prolate anisotropy of a particular ion [16,17], which in turn enables a rational design of molecules with magnetic bistability. Lanthanide ions feature a wide range of different types of magnetic anisotropy. The choice of the most suitable lanthanides depends on the desired properties—Gd(III) is suitable for the construction of qubits or qudits, while the highly anisotropic ions, such as Dy(III) [18,19], Tb(III) [20], Er(III) [21] or Yb(III) [22] are perfect for the construction of SMMs. However, the design of SMMs also requires a careful choice of the ligand scaffold and the solvent. Successful combination of these three components may lead not only to exceptional SMMs, but also to multifunctionality, with multiple co-existing or strongly interacting physical and chemical properties [23]. Chiral SMMs are among the most popular targets as potential multifunctional molecular materials [24–26]. Nevertheless, the combination of magnetism with other properties is often also pursued, which include the following: ferroelectricity [26,27], conductivity [28], luminescence [29–32], optical activity, non-linear optics [33] or redox activity [32]. Helicenes appear to be particularly suited for the design and synthesis of chiral molecule-based magnets. The major limitation, however, is their commercial unavailability as well as their time-consuming and troublesome preparation. This might be the reason why helicenes are so scarcely used for the preparation of chiral SMMs, including Ln-SMMs, as compared to chiral carbon-based ligands [34]. Another reason for a very limited number of such compounds is probably the currently explored synthetic strategy employing an exclusively classical coordination chemistry approach. Coordination chemistry requires the presence of suitable donor atoms in the aromatic backbone of helicenes, which adds to their already troublesome multi-step preparation. Exploration of the π -donor capabilities of helicenes [35–37] demonstrated for *d*-metals might be an interesting alternative, potentially leading to lanthanide–helicene metallocenes.

Lanthanide complexes with helicenes are also interesting from the point of view of luminescence. Lanthanides have very sharp emission lines and usually long lifetimes of the excited states with a variety of available emission energies from visible to near IR. Due to the fact that *f-f* electronic transitions are forbidden (Laporte rule) [38], various ligands are used in lanthanide complexes as antennae for their indirect sensitization [39–43]. Helicenes can also act as antennas, as they consist of conjugated aromatic rings similarly to many ligands with a similar use. Lanthanide complexes with helicenes may also give access to circularly polarized luminescence (CPL), which is much more widely studied for purely organic compounds and transition metal complexes [44–48].

As aforementioned, Ln complexes with helicenes have great potential to exhibit magneto–optical cross-effects such as strong magneto-chiral dichroism (MChD), which stems from the interaction of the unpolarized light with magnetized chiral matter. Depending on the chirality (right or left enantiomer) and the relative orientation of the magnetic field and the light beam (parallel or antiparallel), opposite signals in absorption or emission of light can be observed. In contrast to the natural circular dichroism (NCD) and the magnetic circular dichroism (MCD), which require circularly polarized light, MChD can be observed using unpolarized light—a major benefit from the point of view of future applications. On the other hand, MChD signals are often much weaker than NCD and MCD, but in the case of Ln-helicene complexes the MChD is expected to be significantly stronger.

The theory of MChD was proposed in 1984 [49], but the very first prediction of this cross-effect between natural optical activity (NOA) and magnetic optical activity (MOA) appeared much earlier—in 1962 [50]. The first experimental observation of the MChD effect, however, was reported in 1997 for a chiral lanthanide complex $\text{Eu}(\pm)\text{tfc}_3$ by Rikken and Raupach [51]. Hereafter, a few more examples of MChD have appeared in the literature, such as chiral ferromagnets [52], single chain magnets [53,54], mixed rare-earth/transition-metal clusters [55] and supramolecular aggregates [56]. The theory of MChD predicts strong effects in the case of *f-f* transitions of lanthanides (in the easily accessible UV–vis–IR range) [49], which should be further enhanced by including enantiopure helicenes in the coordination sphere of the complex. Investigation of MChD is important from a

technological point of view, as the optical readout of the magnetization was proposed in compounds showing this property [57,58]. Moreover, MChD is also suspected to be at the origin of the homochirality of life [59–62]. This prompts the full-scale exploration of new lanthanide–helicene complexes as candidates showing strong MChD effect. Herein, we provide an overview of all lanthanide–helicene complexes reported to date and draw conclusions regarding the future direction in this exciting subfield of molecular magnetism.

2. State-of-the-Art—Co-Existence of Chirality, Magnetism and/or Luminescence

In contrast to a very rich family of helicene-based transition metal complexes [63], the number of the corresponding lanthanide complexes is quite limited. Consequently, only a few helicenes were used for the preparation of Ln(III) coordination compounds and were mostly derivatives of 2,2′-bipyridine. Figure 1 gathers all helicenes used so far in the preparation of lanthanide complexes. Such a narrow group of ligands with a very limited number of coordination modes barely scratches the surface of the possible electronic and magnetic interactions between lanthanides and helicenes, but already demonstrates the potential of this type of compound for the construction of multifunctional molecular systems. Apart from helicenes with conventional donor atoms, which enables the classical coordination to lanthanides (Figure 1), the η^5 - and η^6 -helicenic ligands as well as helicenes decorated with alkynyl and vinyl groups were never used for the preparation of ‘organometallic’ lanthanide complexes.

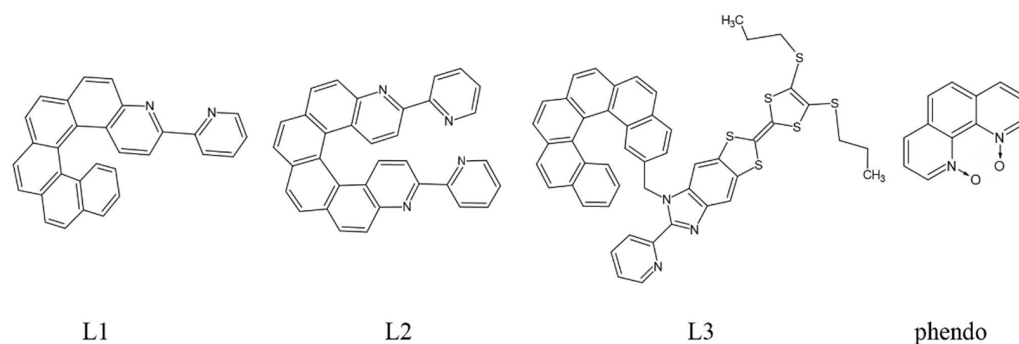


Figure 1. Helicenes used as ligands in the lanthanide-based complexes reported to date: L1 = 3-(2-pyridyl)-4-aza[6]helicene [64], L2 = 3,14-di-(2-pyridyl)-4,13-diaza[6]helicene [65], L3 = 2-{1-[2-methyl[6]helicene]-4,5-[4,5-bis(propylthio)tetrathiafulvalenyl]-1H-benzimidazol-2-yl}pyridine [66] and phendo = 1,10-phenanthroline-*N,N'*-dioxide [67].

All structurally characterized lanthanide complexes with helicene 2,2′-bipyridyl derivatives or *N,N'*-dioxophenanthroline as ligands are collected in Table 1 and described below.

The first lanthanide-based compound from the family of helicene 2,2′-bipyridine derivatives was described in 2016 by Ou-Yang et al. [68]. A mononuclear complex [Dy(hfac)₃(L1)] (**1**) (L1 = 3-(2-pyridyl)-4-aza[6]helicene, hfac[−] = 1,1,1,5,5,5-hexafluoroacetylacetonate) was obtained in a racemic form *rac-1* [Dy(hfac)₃(*rac*-L1)] 0.5C₆H₁₄ (Figure 2) and as pure enantiomers [Dy(hfac)₃(*P*)-L1] **1P** and [Dy(hfac)₃(*M*)-L1] **1M**. The N₂O₆ coordination spheres of the Dy^{III} centers are similar for the racemate *rac-1* and the enantiomers **1P** and **1M** with the geometry of a triangular dodecahedron (*D*_{2d}). However, the crystal packing differs significantly. The racemic form *rac-1* crystallizes in a triclinic space group *P* $\bar{1}$ while pure enantiomers **1P** and **1M** crystallize in a non-centrosymmetric space group *P*2₁2₁2₁. In the case of *rac-1*, the individual molecules are organized in heterochiral supramolecular pairs, whereas in pure enantiomeric forms a helical supramolecular chain arrangement is found due to the specific π - π stacking interactions of the helicene ligands. The completely different crystal packing for *rac-1* and **1P**/**1M** results in different shortest Dy⋯Dy distances: 8.789 Å for *rac-1* and 10.127 Å for **1P** and **1M**. This leads to different magnetic properties for *rac-1* and the pure enantiomers with the opening of the magnetic hysteresis loop for **1P**

and **1M** at 0.5 K. The different crystal packing results in different intermolecular magnetic interactions: Antiferromagnetic for *rac*-**1** and ferromagnetic for pure enantiomers. This was the first report of the different magnetic behavior and slow relaxation of the magnetization of pure chiral SMM enantiomers as compared to their racemic form. However, the influence of the chirality of the helicene on the magnetic properties of the lanthanide in $[\text{Dy}(\text{hfac})_3(\text{L1})]$ (**1**) is steric in nature rather than electronic.

Table 1. A chronological summary of all published lanthanide-helicene complexes characterized structurally, with the CCDC numbers referring to their crystal structures deposited with the Cambridge Structural Database (CSD). The CSD database was searched using the WebCSD tool on 7 July 2021.

Compound Number	Compound	Ln^{III} Ion	CCDC	Structural Formula	Ref.
1	$[\text{Dy}(\text{hfac})_3(\text{L1})]$ (<i>rac</i> - 1 , 1P and 1M) L1 = 3-(2-pyridyl)-4-aza[6]helicene; hfac [−] = 1,1,1,5,5,5-hexafluoroacetylacetonate P and M letters in the acronyms 1P and 1M denote the two enantiomers of the ligand L1 with (<i>P</i>) and (<i>M</i>) helicity, respectively	Dy	1511876 1511877 1511878		[68]
2	$[\text{Dy}(\text{tta})_3(\text{L1})]$ tta [−] = 2-thenoyltrifluoroacetate	Dy	1510324		[69]
3	$[\text{Dy}_2(\text{hfac})_6(\text{L2})]$ L2 = 3,14-di-(2-pyridyl)-4,13-diaza[6]helicene ligand	Dy	1854828		[65]
4	$[\text{Yb}_2(\text{hfac})_6(\text{L2})] \cdot \text{C}_6\text{H}_{14}$	Yb	1854829		[65]

Table 1. Cont.

Compound Number	Compound	Ln ^{III} Ion	CCDC	Structural Formula	Ref.
5, 6, 7, 8	Ln(hfac) ₃ (L1)·0.5C ₆ H ₁₄	Y, Eu, Gd, Yb	1858744 (Yb) 1858745 (Eu) 1858746 (Y) 1858747 (Gd)		[70]
9	[Dy(hfac) ₃ (L3)]·0.5CH ₂ Cl ₂ L3 = 2-[1-[2-methyl[6]helicene]-4,5- [4,5- bis(propylthio)tetrathiafulvalenyl]- 1H-benzimidazol- 2-yl]pyridine	Dy	1867478		[66]
10	[Ln(phendo) ₄](NO ₃) ₃ ·xMeOH phendo = 1,10-phenanthroline- N,N'-dioxide	Gd	1944789 1944790		[71]
11, 12	[Ln(phendo) ₄](NO ₃) ₃ ·xMeOH	Er, Yb	1965558 1965559 1965560 1965556		[72]
8	[Yb(hfac) ₃ (L1)] (8P and 8M) P and M letters in the acronyms 1P and 1M denote the two enantiomers of the ligand L1 with (P) and (M) helicity, respectively	Yb	2049025 2049026		[73]

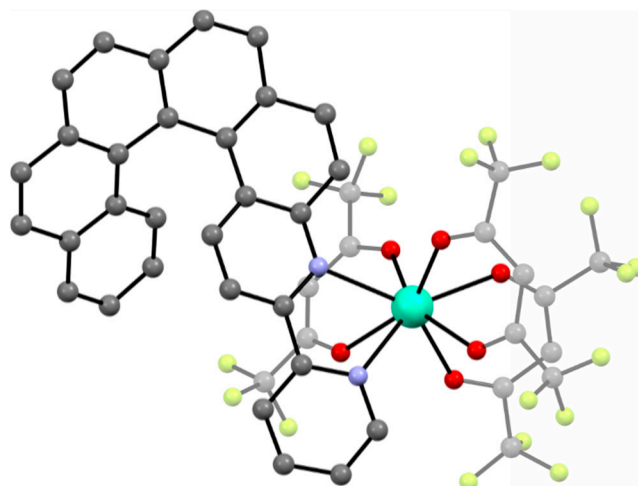


Figure 2. The crystal structure of $[\text{Dy}(\text{hfac})_3(\text{L1})]$ (**1**) as the representative example of the isostructural series $[\text{Ln}(\text{hfac})_3(\text{L1})]$ ($\text{Ln} = \text{Dy}$ for **1**, Y for **5**, Eu for **6**, Gd for **7** and Yb for **8**). Dy—teal, O—red, C—gray, N—blue, F—bright yellow.

The second compound $[\text{Dy}(\text{tta})_3(\text{L1})]$ (**2**) ($\text{tta}^- = 2\text{-thenoyltrifluoroacetate}$ anion) was also published in 2016 [69]. $[\text{Dy}(\text{tta})_3(\text{L1})]$ (**2**) is quite similar to **1** in terms of the first coordination sphere of Dy^{III} and the use of the same helicene ligand L1. The only difference is the use of tta^- anions instead of hfac^- (Figure 3). The replacement of hfac^- by tta^- in the racemic **2** (pure enantiomeric forms were not reported) leads to the observation of slow relaxation of the magnetization and magnetic hysteresis loop at 0.50 K as opposed to the lack of SMM behavior in *rac-1*. The racemic **2** crystallizes in a triclinic $P\bar{1}$ space group with the N_2O_6 coordination sphere of Dy^{III} showing approximately D_{4d} symmetry (distorted square antiprism geometry). Similarly to *rac-1*, heterochiral dimers are formed within the crystal structure of **2** due to the presence of intermolecular $\pi\text{-}\pi$ interactions of the 2,2'-bpy moieties of the L1 ligand. The shortest Dy...Dy distance of 8.935 Å is very similar to that found in *rac-1*. Due to the use of the helicene L1 in its racemic form, it is impossible to classify $[\text{Dy}(\text{tta})_3(\text{L1})]$ (**2**) as a lanthanide–helicene complex with either coupling or co-existence of the chirality and magnetism, because this can only be done for pure enantiomers (in racemic mixtures the effects related to chirality cancel out).

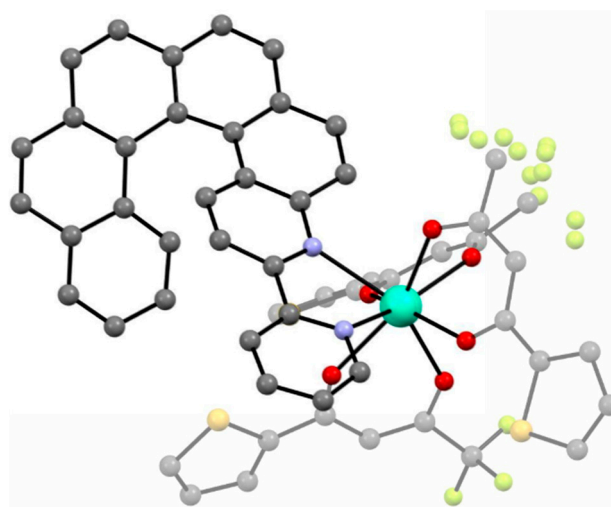


Figure 3. The crystal structure of $[\text{Dy}(\text{tta})_3(\text{L1})]$ (**2**). Dy—teal, O—red, C—gray, N—blue, F—bright yellow, S—yellow.

In 2018, the next two lanthanide–helicene complexes were reported [65]. These two complexes are based on a very similar 2,2′-bipyridyl derivative, but this time it has two 2,2′-bpy fragments, so it can serve as a molecular bridge between two lanthanide ions. Two isostructural compounds are reported: $[\text{Dy}_2(\text{hfac})_6(\text{L2})]$ (**3**) and $[\text{Yb}_2(\text{hfac})_6(\text{L2})]\cdot\text{C}_6\text{H}_{14}$ (**4**) ($\text{L2} = 3,14\text{-di-(2-pyridyl)-4,13-diaza[6]helicene}$) (Figure 4). Only racemic forms of **3** and **4** were obtained and studied. The local geometry of the dinuclear molecules **3** and **4** are very similar, but they differ in the crystal packing due to the presence or absence of the different types of crystallization solvent molecules. Both dimers crystallize in the triclinic $P\bar{1}$ space group. In both dimers every metal center has a slightly different symmetry (two crystallographically independent Dy^{III} or Yb^{III} centers). Helicene angle in the dysprosium dimer **3** is $55.3(1)^\circ$ while in ytterbium dimer **4** it is $61.0(1)^\circ$. Ln⋯Ln distance in **3** and **4** is 9.320 \AA and 9.890 \AA , respectively. Both complexes are field-induced SMMs. Similarly to **1** and **2**, compounds **3** and **4** also show co-existence of the helicene- and lanthanide-specific functionalities, rather than the coupling of the two.

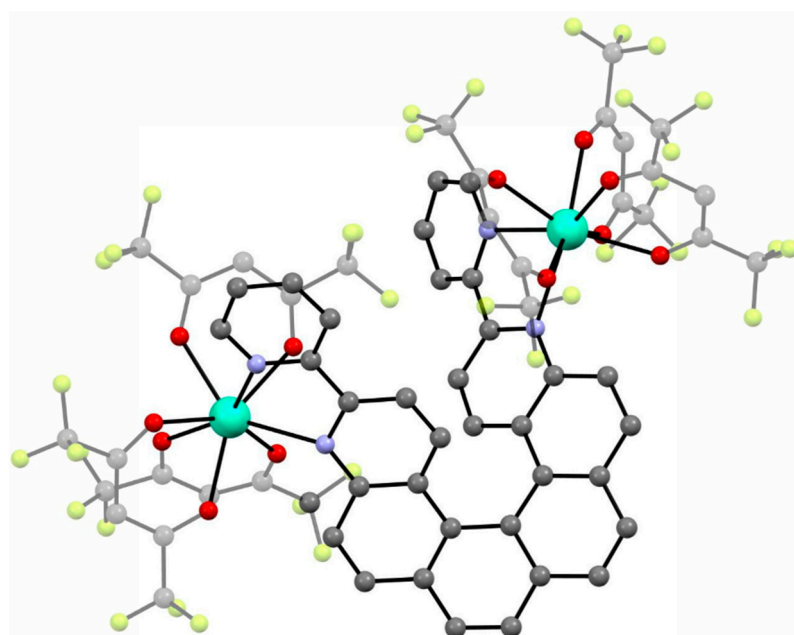


Figure 4. The crystal structure of $[\text{Dy}_2(\text{hfac})_6(\text{L2})]$ (**3**). Dy—teal, O—red, C—gray, N—blue, F—bright yellow. $[\text{Yb}_2(\text{hfac})_6(\text{L2})]\cdot\text{C}_6\text{H}_{14}$ (**4**) shows very similar molecular geometry but different crystal packing.

In 2019 the analogs of *rac-1* with other lanthanide ions were described $[\text{Ln}(\text{hfac})_3(\text{L1})]\cdot 0.5 \text{ C}_6\text{H}_{14}$ ($\text{Ln} = \text{Y}$ (**5**), Eu (**6**), Gd (**7**), Yb (**8**)) [70]. The authors discuss the influence of the Ln center in these isostructural compounds on the enhancement of the singlet oxygen generation and on their luminescence. Ligand L1 was used in this series only in its racemic form. The structures of these four compounds are identical to the Dy-based analog *rac-1*. The shortest Ln⋯Ln distance in these structures is in the $8.694\text{--}8.972 \text{ \AA}$ range.

The detailed analysis of the luminescence was performed for the whole family of compounds and compared with the luminescence of the free ligand. The quantum yield of singlet oxygen generation was also determined for all members of this family. The helicenic ligand L1 itself is a potent single oxygen sensitizer. It was concluded that the coordination of L1 to lanthanide ions could modulate the kinetics of the intersystem crossing and the singlet oxygen generation. Coordination of gadolinium(III) (**7**) significantly improves the singlet oxygen generation in comparison to the free ligand, because gadolinium(III) presents *f-f* transitions much higher in energy than the lowest singlet excited state of the ligand and therefore influences its photophysics solely by the so called “heavy-atom” effect. As no energy transfer from the ligand-centered triplet state to the metal center is energetically allowed, the ligand deactivates by energy transfer to the surrounding

molecular oxygen, resulting in a particularly efficient singlet oxygen photosensitization. In the case of the ytterbium(III) complex (**8**), singlet oxygen sensitization by the ligand simply competes with the energy transfer to the ytterbium center. Finally, coordination to europium(III) decreases the singlet oxygen generation efficiency as compared to the free ligand. Overall, the behavior of $[\text{Eu}(\text{hfac})_3(\text{L1})]$ (**6**) is more complex and leads to faster kinetics of the nonradiative processes, resulting in poor singlet oxygen generation and luminescence. Unfortunately, due to the use of the racemic L1 in the synthesis of **5–8**, it is impossible to assess the influence of the chirality of the heli-cenic L1 on the properties of these complexes.

In 2019, another Dy(III) complex with a more sophisticated heli-cenic ligand was reported by Pointillart et al. [66]. The authors successfully combined the chiral carbo[6]helicene backbone with the electroactive tetrathiafulvalene (TTF) core (L3 in Figure 1). The resulting compound $[\text{Dy}(\text{hfac})_3(\text{L3})] \cdot 0.5\text{CH}_2\text{Cl}_2$ (**9**) (Figure 5) is a chiral redox-active SMM. Only the racemic form of this complex was studied; **9** crystallizes in a triclinic space group $P\bar{1}$. The coordination sphere of Dy(III) N_2O_6 is very similar to the other complexes, **1–8**. The two nitrogen and six oxygen atoms form a *quasi- D_{2d}* polyhedron around the Dy(III) center. The shortest Dy...Dy distance is 9.529 Å. The $[\text{Dy}(\text{hfac})_3(\text{L3})]$ molecules are stacked along the *a* crystallographic axis thanks to the intramolecular π - π interactions between the helicene backbones of one molecule and the (1*H*-benzimidazol-2-yl)pyridine (bzip) fragment of the neighboring one in a “head-to-tail” fashion.

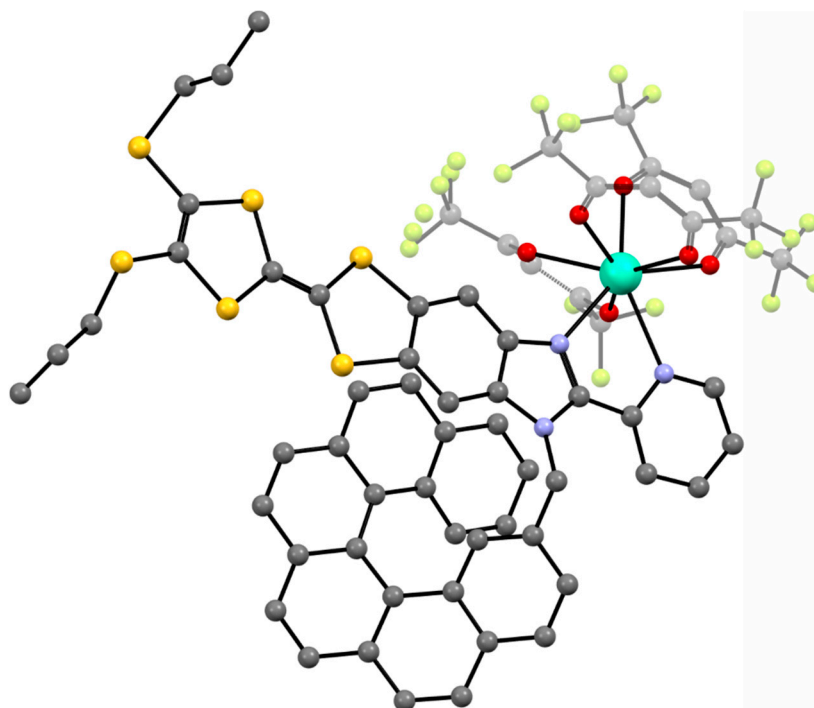


Figure 5. The crystal structure of $[\text{Dy}(\text{hfac})_3(\text{L3})]$ (**9**). Dy—teal, O—red, C—gray, N—blue, F—bright yellow, S—yellow.

Cyclic voltammetry measurements revealed that the redox properties of the ligand L3 are conserved in $[\text{Dy}(\text{hfac})_3(\text{L3})]$ and there are two monoelectronic oxidations: to the radical cation and then to the dication at 0.55 V and 0.94 V. The corresponding oxidation event for the free ligand occurs at 0.53 V and 0.93 V.

[Dy(hfac)₃(L3)] exhibits the slow relaxation of the magnetization, which is driven mainly by the Raman relaxation process. Theoretical calculations (SA-CASSCF/SI-SO) were performed to rationalize the observed magnetic properties and confirm the axial character of the magnetic anisotropy tensor of the ground-state Kramers doublet. According to the calculations, the easy magnetization axis is oriented perpendicular to the plane of the {tetrathiafulvalenyl-1H-benzimidazol-2-yl}pyridine moiety which was also confirmed experimentally by single-crystal magnetic measurements. The synthesis of pure enantiomers of this complex are expected to enable the electrochemical modulation of the circular dichroism signal, optical rotation and SMM behavior of this compound. Nevertheless, at this point there is no direct evidence for coupling between the chirality, magnetism and electrochemistry in [Dy(hfac)₃(L3)].

Recently a homoleptic Gd(III) complex [Gd(phendo)₄](NO₃)₃·xMeOH (**10**) with the smallest helicene-type ligand 1,10-phenanthroline-*N,N'*-dioxide (phendo) was reported by some of us (Figure 6) [71]. The Gd(III) ions in **10** are coordinated solely by four bis-chelating phendo ligands attaining the same helicity and resulting in propeller-shaped complex cations. Due to the very low racemization barrier of phendo, **10** crystallizes in a centrosymmetric tetragonal space group *I4/m* with both left- and right-handed [Gd(phendo)₄]³⁺ propellers in the structure.

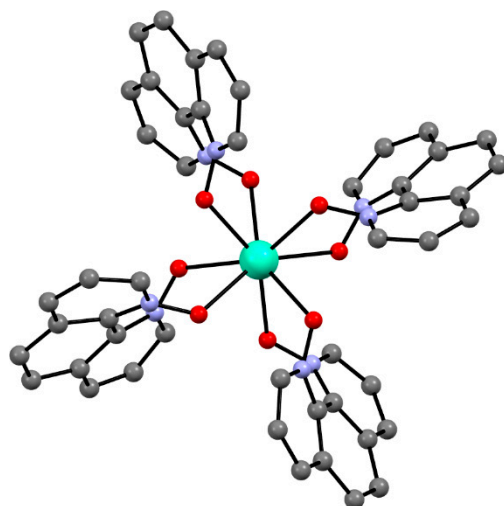


Figure 6. The crystal structure of the [Gd(phendo)₄]³⁺ cation in compound **10** as the representative example of the isostructural series [Ln(phendo)₄](NO₃)₃·xMeOH (Ln = Er for **11**, Yb for **12**). Gd—teal, O—red, C—gray, N—blue.

Detailed magnetic and EPR studies for [Gd(phendo)₄](NO₃)₃·xMeOH (**10**) and its solid state dilutions in the isostructural [Y(phendo)₄](NO₃)₃·xMeOH matrix revealed field-induced SMM (quite rare for Gd(III)-based complexes) and molecular qubit behavior. It was found that the slow magnetic relaxation is driven mainly by the Raman-like process with the relaxation time $\tau \propto T^{-3}$. The coherent spin state manipulation of [Gd(phendo)₄]³⁺ was demonstrated by recording Rabi oscillations at temperatures as high as 20 K.

The propeller-shaped analogs of [Gd(phendo)₄](NO₃)₃·xMeOH (**10**) with Er (**11**) and Yb (**12**), were also obtained and studied [72]. Both [Er(phendo)₄](NO₃)₃·xMeOH (**11**) and [Yb(phendo)₄](NO₃)₃·xMeOH (**12**) exhibit slow magnetic relaxation typical for field-induced SMMs. Detailed magnetic studies of the solid state dilution compounds using [Y(phendo)₄](NO₃)₃·xMeOH as the dilution matrix revealed a similar temperature dependence of the relaxation of the magnetization for **10**, **11** and **12** controlled by a nearly identical Raman process with $\tau \propto T^{-3}$ at lower temperatures. At higher temperatures, **11** and **12** also show a contribution of the Orbach-type relaxation with the estimated energy barrier for the magnetization reversal $U_{\text{eff}}/k_{\text{B}}$ of 44(2) K and 38(1) K, respectively. Similar to **1–9**, compounds **10**, **11** and **12** also do not demonstrate the desired coupling of the unique

chirality of the helicenes with the extraordinary magnetism of the lanthanides, which can only be revealed for pure enantiomeric forms.

3. Towards Coupling of the Helicene's Chirality and Lanthanide's Magnetism

Section 2 reveals that the coupling between the chirality of the helicene ligand and the magnetism of the lanthanide central ion can only be revealed for pure enantiomeric forms. Recently, the racemic compound $[\text{Ln}(\text{hfac})_3(\text{L1})]$ (**8**), discussed in the previous section, was obtained in the form of pure enantiomers ($[\text{Yb}(\text{hfac})_3((P)\text{-L1})]$ **8P** and $[\text{Yb}(\text{hfac})_3((M)\text{-L1})]$ **8M** [73]. These compounds are isostructural with the pure enantiomers **1P** and **1M** of the Dy(III) analog (also discussed in the beginning of the previous section and reported in 2016 [68]). Apart from the pure (*P*) or (*M*) helicity of the ligands L1 in **8P** and **8M**, the Yb(III) centers also show their own axial chirality due to the presence of four bis-chelating ligands: Δ -type in **8P** and Λ -type in **8M**. Alternating current (AC) magnetic susceptibility measurements for **8M** revealed slow magnetic relaxation under the external dc magnetic field—typical for field-induced SMMs.

Isolation of the two enantiomers of $[\text{Yb}(\text{hfac})_3(\text{L1})]$ enabled the detection of the magneto-chiral dichroism (MChD) signal in the near-IR absorption spectroscopy. It is the first example of the MChD effect measured for a helicene-based coordination compound. The fine-structured strong MChD signal in the 920–990 nm range for **8P** and **8M** originates from the difference in absorption of the ${}^2F_{5/2} \leftarrow {}^2F_{7/2}$ electronic transition of Yb(III). Detailed studies of the temperature and magnetic field dependence of the MChD spectra revealed that the narrow signal of the lowest energy (maximum at 980 nm) can be assigned to the $0' \leftarrow 0$ transition between the lowest energy Kramers doublets of the ${}^2F_{7/2}$ and ${}^2F_{5/2}$ states. The temperature and the magnetic field dependencies of the MChD signal $\Delta A_{\text{MChD}}(T)$ and $\Delta A_{\text{MChD}}(H)$ accurately follow the corresponding magnetization dependencies $M(T)$ and $M(H)$, as predicted by the MChD theory [49]. The helical nature of the helicene L1 in $[\text{Yb}(\text{hfac})_3(\text{L1})]$ influences the chiral arrangement of the bis-chelating ligands around the Yb(III) ion, which is directly associated with the MChD effect. This is the first example where the helicene ligand coordinated to a lanthanide ion enables strong magneto-chiral dichroism.

4. Conclusions

The presented review of the lanthanide–helicene complexes shows that there are only five types of molecules reported to date, with only eleven compounds of this type studied in total. Moreover, these complexes were obtained using a classical coordination chemistry approach, where the helicene is equipped with a classical coordination group such as 2,2'-bpy. This is a clear indication that the field is still in its infancy and requires a huge amount of experimental and theoretical work in order to fully understand and take advantage of the possible coupling of the strong chirality of helicenes, with the unique magnetic properties of lanthanides. One of the possible synthetic routes towards Ln-helicene complexes with potentially strong coupling of the chirality and magnetism would be through the use of the π -coordination ability of helicenes, as demonstrated for some *d*-metal complexes. This strategy has not been explored yet and is currently being pursued in our laboratory.

Of note, there are only two examples of Ln-helicene complexes; **1** [68] and **8** [73] were obtained in optically pure forms. Preparation of optically pure Ln-helicene compounds is a fundamental requirement for the observation of the NCD and MChD phenomena in the bulk material, as both effects cancel out in racemic mixtures. The MChD studies of the bulk (crystals or powder) enable the selection of the most promising molecules that could fulfill the promise of the construction of future MChD magneto–optical single-molecule devices based on this class of compounds. Moreover, the practical applications of Ln-helicene compounds depend on the possibility of the observation of the MChD effect above the boiling point of nitrogen and under zero magnetic field—we believe that Ln-helicene SMMs would be able to fulfill this requirement.

Finally, the recent magneto-chiral dichroism (MChD) measurements for an optically pure lanthanide–helicene complex [Yb(hfac)₃(L1)] [73] confirm the theory that the MChD signal is coupled with the magnetization of the metal center. This constitutes an important breakthrough that validates the concept of the optical detection of magnetization in molecular magnets using unpolarized light, as introduced by Train et al. in 2008 [52], and extends it to lanthanide single molecule magnets (Ln-SMMs). Nevertheless, the actual demonstration of the optical readout of a chiral molecular magnet or SMM is still awaited.

Author Contributions: Conceptualization, D.P. and G.H.; data curation, G.H. and K.R.; writing—original draft preparation, G.H. and K.R.; writing—review and editing, D.P., G.H. and K.R.; visualization, G.H. and K.R.; funding acquisition, D.P. and G.H. All authors have read and agreed to the published version of the manuscript.

Funding: Financial support of the National Science Center within the Opus project 2020/37/B/ST5/02735 is gratefully acknowledged. GH acknowledges the Polish Ministry of Science and Higher Education for the Diamond Grant 0191/DIA/2017/46.

Conflicts of Interest: The authors declare no conflict of interest.

References

1. Shen, Y.; Chen, C.-F. Helicenes: Synthesis and Applications. *Chem. Rev.* **2011**, *112*, 1463–1535. [[CrossRef](#)] [[PubMed](#)]
2. Chen, C.-F.; Shen, Y. *Helicene Chemistry*; Springer: Berlin/Heidelberg, Germany, 2017.
3. Gingras, M. One hundred years of helicene chemistry. Part 1: Non-stereoselective syntheses of carbohelicenes. *Chem. Soc. Rev.* **2013**, *42*, 968–1006. [[CrossRef](#)]
4. Gingras, M. One hundred years of helicene chemistry. Part 3: Applications and properties of carbohelicenes. *Chem. Soc. Rev.* **2013**, *42*, 1051–1095. [[CrossRef](#)] [[PubMed](#)]
5. Ou-Yang, J.-K.; Crassous, J. Chiral multifunctional molecules based on organometallic helicenes: Recent advances. *Coord. Chem. Rev.* **2018**, *376*, 533–547. [[CrossRef](#)]
6. Gingras, M.; Félix, G.; Peresutti, R. One hundred years of helicene chemistry. Part 2: Stereoselective syntheses and chiral separations of carbohelicenes. *Chem. Soc. Rev.* **2013**, *42*, 1007–1050. [[CrossRef](#)] [[PubMed](#)]
7. Nakai, Y.; Mori, T.; Inoue, Y. Theoretical and Experimental Studies on Circular Dichroism of Carbo[n]helicenes. *J. Phys. Chem. A* **2012**, *116*, 7372–7385. [[CrossRef](#)] [[PubMed](#)]
8. Otani, T.; Tsuyuki, A.; Iwachi, T.; Someya, S.; Tateno, K.; Kawai, H.; Saito, T.; Kanyiva, K.S.; Shibata, T. Facile Two-Step Synthesis of 1,10-Phenanthroline-Derived Polyaza[7]helicenes with High Fluorescence and CPL Efficiency. *Angew. Chem. Int. Ed.* **2017**, *56*, 3906–3910. [[CrossRef](#)]
9. He, D.-Q.; Lu, H.-Y.; Li, M.; Chen, C.-F. Intense blue circularly polarized luminescence from helical aromatic esters. *Chem. Commun.* **2017**, *53*, 6093–6096. [[CrossRef](#)]
10. Katayama, T.; Nakatsuka, S.; Hirai, H.; Yasuda, N.; Kumar, J.; Kawai, T.; Hatakeyama, T. Two-Step Synthesis of Boron-Fused Double Helicenes. *J. Am. Chem. Soc.* **2016**, *138*, 5210–5213. [[CrossRef](#)] [[PubMed](#)]
11. Goto, K.; Yamaguchi, R.; Hiroto, S.; Ueno, H.; Kawai, T.; Shinokubo, H. Intermolecular Oxidative Annulation of 2-Aminoanthracenes to Diazaacenes and Aza[7]helicenes. *Angew. Chem. Int. Ed.* **2012**, *51*, 10333–10336. [[CrossRef](#)]
12. Ushiyama, A.; Hiroto, S.; Yuasa, J.; Kawai, T.; Shinokubo, H. Synthesis of a figure-eight azahelicene dimer with high emission and CPL properties. *Org. Chem. Front.* **2016**, *4*, 664–667. [[CrossRef](#)]
13. Mannini, M.; Pineider, F.; Sainctavit, P.; Danieli, C.; Otero, E.; Sciancalepore, C.; Talarico, A.M.; Arrio, M.-A.; Cornia, A.; Gatteschi, D.; et al. Magnetic memory of a single-molecule quantum magnet wired to a gold surface. *Nat. Mater.* **2009**, *8*, 194–197. [[CrossRef](#)]
14. Pedersen, K.S.; Ariciu, A.-M.; McAdams, S.; Weihe, H.; Bendix, J.; Tuna, F.; Piligkos, S. Toward Molecular 4f Single-Ion Magnet Qubits. *J. Am. Chem. Soc.* **2016**, *138*, 5801–5804. [[CrossRef](#)]
15. Rocha, A.R.; Suarez, V.M.G.; Bailey, S.W.; Lambert, C.; Ferrer, J.; Sanvito, S. Towards molecular spintronics. *Nat. Mater.* **2005**, *4*, 335–339. [[CrossRef](#)]
16. Rinehart, J.; Long, J.R. Exploiting single-ion anisotropy in the design of f-element single-molecule magnets. *Chem. Sci.* **2011**, *2*, 2078–2085. [[CrossRef](#)]
17. Zhang, P.; Zhang, L.; Tang, J. Lanthanide single molecule magnets: Progress and perspective. *Dalton Trans.* **2015**, *44*, 3923–3929. [[CrossRef](#)] [[PubMed](#)]
18. Goodwin, C.; Ortu, F.; Reta, D.; Chilton, N.F.; Mills, D. Molecular magnetic hysteresis at 60 kelvin in dysprosocenium. *Nature* **2017**, *548*, 439–442. [[CrossRef](#)]
19. Guo, F.-S.; Day, B.M.; Chen, Y.-C.; Tong, M.; Mansikkamäki, A.; Layfield, R.A. A Dysprosium Metallocene Single-Molecule Magnet Functioning at the Axial Limit. *Angew. Chem. Int. Ed.* **2017**, *56*, 11445–11449. [[CrossRef](#)]
20. Ishikawa, N.; Sugita, M.; Ishikawa, T.; Koshihara, S.-Y.; Kaizu, Y. Lanthanide Double-Decker Complexes Functioning as Magnets at the Single-Molecular Level. *J. Am. Chem. Soc.* **2003**, *125*, 8694–8695. [[CrossRef](#)] [[PubMed](#)]

21. Zhang, P.; Zhang, L.; Wang, C.; Xue, S.; Lin, S.-Y.; Tang, J. Equatorially Coordinated Lanthanide Single Ion Magnets. *J. Am. Chem. Soc.* **2014**, *136*, 4484–4487. [[CrossRef](#)] [[PubMed](#)]
22. Gavrikov, A.V.; Efimov, N.N.; Ilyukhin, A.B.; Dobrokhotova, Z.V.; Novotortsev, V.M. Yb³⁺ can be much better than Dy³⁺: SMM properties and controllable self-assembly of novel lanthanide 3,5-dinitrobenzoate-acetylacetonate complexes. *Dalton Trans.* **2018**, *47*, 6199–6209. [[CrossRef](#)] [[PubMed](#)]
23. Train, C.; Gruselle, M.; Verdaguer, M. The fruitful introduction of chirality and control of absolute configurations in molecular magnets. *Chem. Soc. Rev.* **2011**, *40*, 3297–3312. [[CrossRef](#)]
24. Liu, C.-M.; Zhang, D.-Q.; Zhu, D.-B. Field-Induced Single-Ion Magnets Based on Enantiopure Chiral β -Diketonate Ligands. *Inorg. Chem.* **2013**, *52*, 8933–8940. [[CrossRef](#)] [[PubMed](#)]
25. Inglis, R.; White, F.; Piligkos, S.; Wernsdorfer, W.; Brechin, E.; Papaefstathiou, G. Chiral single-molecule magnets: A partial Mn(III) supertetrahedron from achiral components. *Chem. Commun.* **2011**, *47*, 3090–3092. [[CrossRef](#)] [[PubMed](#)]
26. Long, J.; Rouquette, J.; Thibaud, J.-M.; Ferreira, R.; Carlos, L.; Donnadiou, B.; Vieru, V.; Chibotaru, L.; Konczewicz, L.; Haines, J.; et al. A High-Temperature Molecular Ferroelectric Zn/Dy Complex Exhibiting Single-Ion-Magnet Behavior and Lanthanide Luminescence. *Angew. Chem. Int. Ed.* **2014**, *54*, 2236–2240. [[CrossRef](#)] [[PubMed](#)]
27. Wang, Y.-X.; Shi, W.; Li, H.; Song, Y.; Fang, L.; Lan, Y.; Powell, A.K.; Wernsdorfer, W.; Ungur, L.; Chibotaru, L.F.; et al. A single-molecule magnet assembly exhibiting a dielectric transition at 470 K. *Chem. Sci.* **2012**, *3*, 3366–3370. [[CrossRef](#)]
28. Coronado, E.; Day, P. Magnetic Molecular Conductors. *Chem. Rev.* **2004**, *104*, 5419–5448. [[CrossRef](#)]
29. Pedersen, K.S.; Dreiser, J.; Weihe, H.; Sibille, R.; Johannesen, H.V.; Sørensen, M.A.; Nielsen, B.E.; Sigrist, M.; Mutka, H.; Rols, S.; et al. Design of Single-Molecule Magnets: Insufficiency of the Anisotropy Barrier as the Sole Criterion. *Inorg. Chem.* **2015**, *54*, 7600–7606. [[CrossRef](#)]
30. Long, J.; Vallat, R.; Ferreira, R.A.S.; Carlos, L.D.; Paz, F.A.A.; Guari, Y.; Larionova, J. A bifunctional luminescent single-ion magnet: Towards correlation between luminescence studies and magnetic slow relaxation processes. *Chem. Commun.* **2012**, *48*, 9974–9976. [[CrossRef](#)]
31. Pointillart, F.; Le Guennic, B.; Golhen, S.; Cador, O.; Maury, O.; Ouahab, L. A redox-active luminescent ytterbium based single molecule magnet. *Chem. Commun.* **2013**, *49*, 615–617. [[CrossRef](#)]
32. Pointillart, F.; le Guennic, B.; Cador, O.; Maury, O.; Ouahab, L. Lanthanide Ion and Tetrathiafulvalene-Based Ligand as a “Magic” Couple toward Luminescence, Single Molecule Magnets, and Magnetostructural Correlations. *Acc. Chem. Res.* **2015**, *48*, 2834–2842. [[CrossRef](#)]
33. Train, C.; Nuida, T.; Gheorghe, R.; Gruselle, M.; Ohkoshi, S.-I. Large Magnetization-Induced Second Harmonic Generation in an Enantiopure Chiral Magnet. *J. Am. Chem. Soc.* **2009**, *131*, 16838–16843. [[CrossRef](#)]
34. Aspinall, H.C. Chiral Lanthanide Complexes: Coordination Chemistry and Applications. *Chem. Rev.* **2002**, *102*, 1807–1850. [[CrossRef](#)]
35. Katz, T.J.; Pesti, J. The synthesis of a helical ferrocene. *J. Am. Chem. Soc.* **1982**, *104*, 346–347. [[CrossRef](#)]
36. Fuchter, M.; Schaefer, J.; Judge, D.K.; Wardzinski, B.; Weimar, M.; Krossing, I. [7]-Helicene: A chiral molecular tweezer for silver(I) salts. *Dalton Trans.* **2012**, *41*, 8238. [[CrossRef](#)]
37. Akiyama, M.; Nozaki, K. Synthesis of Optically Pure Helicene Metallocenes. *Angew. Chem. Int. Ed.* **2017**, *56*, 2040–2044. [[CrossRef](#)] [[PubMed](#)]
38. Van Vleck, J.H. The Puzzle of Rare-earth Spectra in Solids. *J. Phys. Chem.* **1937**, *41*, 67–80. [[CrossRef](#)]
39. Heffern, M.C.; Matosziuk, L.M.; Meade, T.J. Lanthanide Probes for Bioresponsive Imaging. *Chem. Rev.* **2013**, *114*, 4496–4539. [[CrossRef](#)] [[PubMed](#)]
40. Wang, X.; Chang, H.; Xie, J.; Zhao, B.; Liu, B.; Xu, S.; Pei, W.; Ren, N.; Huang, L.; Huang, W. Recent developments in lanthanide-based luminescent probes. *Coord. Chem. Rev.* **2014**, *273–274*, 201–212. [[CrossRef](#)]
41. Hasegawa, Y.; Kitagawa, Y.; Nakanishi, T. Effective photosensitized, electrosensitized, and mechanosensitized luminescence of lanthanide complexes. *NPG Asia Mater.* **2018**, *10*, 52–70. [[CrossRef](#)]
42. Bünzli, J.-C.G.; Piguet, C. Taking advantage of luminescent lanthanide ions. *Chem. Soc. Rev.* **2005**, *34*, 1048–1077. [[CrossRef](#)]
43. Zakrzewski, J.J.; Chorazy, S.; Nakabayashi, K.; Ohkoshi, S.; Sieklucka, B. Photoluminescent Lanthanide(III) Single-Molecule Magnets in Three-Dimensional Polycyanidocuprate(I)-Based Frameworks. *Chem. Eur. J.* **2019**, *25*, 11820–11825. [[CrossRef](#)]
44. Zhao, W.-L.; Li, M.; Lu, H.-Y.; Chen, C.-F. Advances in helicene derivatives with circularly polarized luminescence. *Chem. Commun.* **2019**, *55*, 13793–13803. [[CrossRef](#)] [[PubMed](#)]
45. Kubo, H.; Hirose, T.; Nakashima, T.; Kawai, T.; Hasegawa, J.-Y.; Matsuda, K. Tuning Transition Electric and Magnetic Dipole Moments: [7]Helicenes Showing Intense Circularly Polarized Luminescence. *J. Phys. Chem. Lett.* **2021**, *12*, 686–695. [[CrossRef](#)] [[PubMed](#)]
46. Dhbaibi, K.; Shen, C.; Jean, M.; Vanthuyne, N.; Roisnel, T.; Górecki, M.; Jamoussi, B.; Favereau, L.; Crassous, J. Chiral Diketopyrrolopyrrole-Helicene Polymer with Efficient Red Circularly Polarized Luminescence. *Front. Chem.* **2020**, *8*, 237. [[CrossRef](#)] [[PubMed](#)]
47. Lunkley, J.L.; Shirota, D.; Yamanari, K.; Kaizaki, S.; Muller, G. Extraordinary Circularly Polarized Luminescence Activity Exhibited by Cesium Tetrakis(3-heptafluoro-butylryl(+)-camphorato) Eu(III) Complexes in EtOH and CHCl₃ Solutions. *J. Am. Chem. Soc.* **2008**, *130*, 13814–13815. [[CrossRef](#)] [[PubMed](#)]

48. Carr, R.; Evans, N.; Parker, D. Lanthanide complexes as chiral probes exploiting circularly polarized luminescence. *Chem. Soc. Rev.* **2012**, *41*, 7673–7686. [[CrossRef](#)]
49. Barron, L.; Urbancich, J. Magneto-chiral birefringence and dichroism. *Mol. Phys.* **1984**, *51*, 715–730. [[CrossRef](#)]
50. Groenewege, M. A theory of magneto-optical rotation in diamagnetic molecules of low symmetry. *Mol. Phys.* **1962**, *5*, 541–563. [[CrossRef](#)]
51. Rikken, G.L.J.A.; Raupach, E. Observation of magneto-chiral dichroism. *Nature* **1997**, *390*, 493–494. [[CrossRef](#)]
52. Train, C.; Gheorghie, R.; Krstic, V.; Chamoreau, L.-M.; Ovanesyan, N.S.; Rikken, G.L.J.A.; Gruselle, M.; Verdaguer, M. Strong magneto-chiral dichroism in enantiopure chiral ferromagnets. *Nat. Mater.* **2008**, *7*, 729–734. [[CrossRef](#)]
53. Sessoli, R.; Boulon, M.-E.; Caneschi, A.; Mannini, M.; Poggini, L.; Wilhelm, F.; Rogalev, A. Strong magneto-chiral dichroism in a paramagnetic molecular helix observed by hard X-rays. *Nat. Phys.* **2014**, *11*, 69–74. [[CrossRef](#)] [[PubMed](#)]
54. Atzori, M.; Santanni, F.; Breslavetz, I.; Paillot, K.; Caneschi, A.; Rikken, G.L.J.A.; Sessoli, R.; Train, C. Magnetic Anisotropy Drives Magnetochiral Dichroism in a Chiral Molecular Helix Probed with Visible Light. *J. Am. Chem. Soc.* **2020**, *142*, 13908–13916. [[CrossRef](#)]
55. Ceolín, M.; Goberna-Ferrón, S.; Galán-Mascarós, J.R. Strong Hard X-ray Magnetochiral Dichroism in Paramagnetic Enantiopure Molecules. *Adv. Mater.* **2012**, *24*, 3120–3123. [[CrossRef](#)]
56. Kitagawa, Y.; Segawa, H.; Ishii, K. Magneto-Chiral Dichroism of Organic Compounds. *Angew. Chem. Int. Ed.* **2011**, *50*, 9133–9136. [[CrossRef](#)]
57. Barron, L.D. Chirality, magnetism and light. *Nature* **2000**, *405*, 895–896. [[CrossRef](#)]
58. Galán-Mascarós, J.R. Bring to light. *Nat. Phys.* **2015**, *11*, 7–8. [[CrossRef](#)]
59. Wagnière, G.H. *On Chirality and the Universal Asymmetry: Reflections on Image and Mirror Image*; Wiley-VCH Verlag GmbH & Co. KGaA: Weinheim, Germany, 2007.
60. Guijarro, A.; Yus, M. *The Origin of Chirality in the Molecules of Life*; Royal Society of Chemistry: Cambridge, UK, 2008. [[CrossRef](#)]
61. Atzori, M.; Rikken, G.L.J.A.; Train, C. Magneto-Chiral Dichroism: A Playground for Molecular Chemists. *Chem. Eur. J.* **2020**, *26*, 9784–9791. [[CrossRef](#)] [[PubMed](#)]
62. Ishii, K.; Hattori, S.; Kitagawa, Y. Recent advances in studies on the magneto-chiral dichroism of organic compounds. *Photochem. Photobiol. Sci.* **2019**, *19*, 8–19. [[CrossRef](#)]
63. Saleh, N.; Shen, C.; Crassous, J. Helicene-based transition metal complexes: Synthesis, properties and applications. *Chem. Sci.* **2014**, *5*, 3680–3694. [[CrossRef](#)]
64. Saleh, N.; Moore, B.; Srebro-Hooper, M.; Vanthuyne, N.; Toupet, L.; Williams, J.A.G.; Roussel, C.; Deol, K.K.; Muller, G.; Autschbach, J.; et al. Acid/Base-Triggered Switching of Circularly Polarized Luminescence and Electronic Circular Dichroism in Organic and Organometallic Helicenes. *Chem. Eur. J.* **2014**, *21*, 1673–1681. [[CrossRef](#)]
65. Flores Gonzalez, J.; Montigaud, V.; Saleh, N.; Cador, O.; Crassous, J.; Le Guennic, B.; Pointillart, F. Slow Relaxation of the Magnetization in Bis-Decorated Chiral Helicene-Based Coordination Complexes of Lanthanides. *Magnetochemistry* **2018**, *4*, 39. [[CrossRef](#)]
66. Pointillart, F.; Ou-Yang, J.-K.; Garcia, G.F.; Montigaud, V.; Gonzalez, J.F.; Marchal, R.; Favereau, L.; Totti, F.; Crassous, J.; Cador, O.; et al. Tetrathiafulvalene-Based Helicene Ligand in the Design of a Dysprosium Field-Induced Single-Molecule Magnet. *Inorg. Chem.* **2018**, *58*, 52–56. [[CrossRef](#)]
67. Rozen, S.; Dayan, S. At Last, 1,10-Phenanthroline-N,N'-dioxide, A New Type of Helicene, has been Synthesized using HOF-CH₃CN. *Angew. Chem. Int. Ed.* **1999**, *38*, 3471–3473. [[CrossRef](#)]
68. Ou-Yang, J.K.; Saleh, N.; Fernandez Garcia, G.; Norel, L.; Pointillart, F.; Guizouarn, T.; Cador, O.; Totti, F.; Ouahab, L.; Crassous, J.; et al. Improved slow magnetic relaxation in optically pure helicene-based Dy(III) single molecule magnets. *Chem. Commun.* **2016**, *52*, 14474–14477. [[CrossRef](#)]
69. Fernandez-Garcia, G.; Gonzalez, J.F.; Ou-Yang, J.-K.; Saleh, N.; Pointillart, F.; Cador, O.; Guizouarn, T.; Totti, F.; Ouahab, L.; Crassous, J.; et al. Slow Magnetic Relaxation in Chiral Helicene-Based Coordination Complex of Dysprosium. *Magnetochemistry* **2016**, *3*, 2. [[CrossRef](#)]
70. Galland, M.; Riobé, F.; Ouyang, J.; Saleh, N.; Pointillart, F.; Dorcet, V.; Le Guennic, B.; Cador, O.; Crassous, J.; Andraud, C.; et al. Helicenic Complexes of Lanthanides: Influence of the f-Element on the Intersystem Crossing Efficiency and Competition between Luminescence and Oxygen Sensitization. *Eur. J. Inorg. Chem.* **2019**, *2019*, 118–125. [[CrossRef](#)]
71. Handzlik, G.; Magott, M.; Arczyński, M.; Sheveleva, A.; Tuna, F.; Sarewicz, M.; Osyczka, A.; Rams, M.; Vieru, V.; Chibotaru, L.F.; et al. Magnetization Dynamics and Coherent Spin Manipulation of a Propeller Gd(III) Complex with the Smallest Helicene Ligand. *J. Phys. Chem. Lett.* **2020**, *11*, 1508–1515. [[CrossRef](#)] [[PubMed](#)]
72. Handzlik, G.; Magott, M.; Arczyński, M.; Sheveleva, A.; Tuna, F.; Baran, S.; Pinkowicz, D. Identical anomalous Raman relaxation exponent in a family of single ion magnets: Towards reliable Raman relaxation determination? *Dalton Trans.* **2020**, *49*, 11942–11949. [[CrossRef](#)] [[PubMed](#)]
73. Atzori, M.; Dhbaibi, K.; Douib, H.; Grasser, M.; Dorcet, V.; Breslavetz, I.; Paillot, K.; Cador, O.; Rikken, G.L.J.A.; Le Guennic, B.; et al. Helicene-Based Ligands Enable Strong Magneto-Chiral Dichroism in a Chiral Ytterbium Complex. *J. Am. Chem. Soc.* **2021**, *143*, 2671–2675. [[CrossRef](#)]